Astron. Astrophys. 322, 825–834 (1997)

ASTRONOMY
AND
ASTROPHYSICS

The distance to the T Tauri stars in Taurus determined from their rotational properties

Thomas Preibisch and Michael D. Smith

Astronomisches Institut der Universität Würzburg, Am Hubland, D-97074 Würzburg, Germany

Received 22 July 1996 / Accepted 12 December 1996

Abstract. We have determined the average distance to the young stars in the Taurus star formation region through their rotational properties. While most other distance estimates to star forming regions give the distance to the associated molecular clouds, the method used here gives the distance to the stars. Our statistical method assumes that the photometric variations are due to surface starspots that co-rotate with the equatorial surface speed and the rotation axes of the stars are randomly distributed. Furthermore, we pay much attention to possible unresolved binaries. A "best fit" distance of 152 $\pm$ 10 parsecs is derived from our sample of 25 weak line T Tauri stars in Taurus. This is within the range of distances found for the molecular cloud (140 pc – 160 pc) and confirms that the T Tauri stars are embedded within.

Alternatively, the agreement of the distances to the stars and dark cloud, along with their intimate sky location, lends support to the interpretation and assumptions. This means that we find a random orientation of the rotation axes, which excludes a preferential orientation that might be caused by large scale magnetic fields in the molecular cloud. Another aspect is that our results seem to exclude strong differential rotation for the T Tauri stars.

Key words: methods: statistical – stars: pre-main-sequence – stars: rotation – stars: distances – ISM: Taurus clouds

1. Introduction

To date, we have no first-hand information on the distance to associations of T Tauri stars (TTS). Instead, it is assumed that they are still embedded in the dark cloud, the distance to which can be estimated through other stars with properties which allow their distances and relationship to the cloud to be unequivocally determined (Elias 1978). This roundabout route is not altogether satisfactory, especially since molecular clouds can have a significant depth. Since for many young stars it is not known whether they are located at the near side of the cloud, at the far side, or at the center, there is a severe uncertainty in the distance. This may cause serious errors, e.g. as remarked by Gomez et al. (1992), if the age of the stars is to be inferred from their positions in the HR diagram.

We use here a statistical method to directly obtain the average distance to a group of stars (which then of course also yields the cloud distance). This method, described below, takes the explanation for the origin of the periodic light-curve variations of TTS as large surface features which rotate with the stellar rotational velocity. The distance is deduced on comparing these photometric periods with spectroscopically-derived values for the rotational velocity. We note that a similar method has been presented by Hendry et al. (1993) and used by O'Dell et al. (1994) to determine the distances to the Pleiades and the α Persei clusters. The method we use in this study has the same foundations but uses a different approach to determine the distance.

In this study we will consider the stars associated with the Taurus molecular cloud, a nearby low-mass star formation region which has been well-studied (cf. Kenyon & Hartmann 1995; Neuhäuser et al. 1995). The Taurus cloud contains several hundred pre-main sequences stars and is the only region in which the rotational properties of a sufficient number of objects are known at present, mostly from the COYOTES studies of Bouvier et al. (1993, 1995). Elias (1978) and Kenyon et al. (1994) have summarized all serious attempts to determine the distance to the cloud complex. Foreground and background stars can be recognized by the difference in reddening to infer an approximate distance of 140$\pm$10 pc. A second method employs the inference that a few stars are associated with the dark cloud because they have reflection nebulosity in their vicinity as supported by their clustering around OB and T associations (Racine 1968). Elias (1978) lists four such stars from which a distance of 135 $\pm$ 15 pc was derived.

Recently-quoted values for the distance to the Taurus TTS seem to be based on personal preference with the provision that, to within 20%, it doesn't really matter. Thus, as examples, Strom et al. (1989), Bouvier et al. (1993, 1995) and Valenti et al. (1993) take 160 pc, Eislöffel (1992) takes 150 pc, Walter et al. (1988) and Leinert et al. (1993) 140 pc and Cernicharo et

Send offprint requests to: Th. Preibisch

al. (1985) 135 pc. However, if one tries to estimate stellar ages from the position of the stars in the HR diagram by comparison with evolutionary tracks, e.g from D'Antona & Mazzitelli (1994), the assumption of either 140 pc or 160 pc can cause age differences of up to a factor of two.

So it would be clearly advantageous, to determine the distances for the T Tauri stars directly and to better accuracy than 20 pc. The method we use here is able to provide such a distance estimate.

2. The stellar sample

The method we introduce in the next section requires three pieces of information about each star: the photometric period P, the spectroscopic-derived velocity component $v \sin i$ and the stellar angular diameter ϕ. All data for our sample are summarized in Table 1.

We have restricted our sample to 'weak-line' T Tauri stars (WTTS). We did not include any classical T Tauri stars (CTTS) for the following reasons. Many CTTS are surrounded by a rather large amount of circumstellar material and show evidence for accretion processes (cf. Montmerle 1990). This often causes large excesses in the ultraviolet as well as the infrared region of the spectral energy distribution of the CTTS (cf. Bouvier & Bertout 1992) and it is often very difficult, if not impossible, to disentangle the radiation originating in the photosphere of the CTTS from that originating from the accretion shock or an active disk. This can cause large errors in the determination of the stellar luminosity and causes correspondingly large errors when trying to determine the stellar radius. Furthermore, the periodic lightcurves of CTTS in many cases suggest the presence of 'hot spots' that are probably related to accretion of circumstellar material onto the stellar surface (cf. Bouvier et al. 1995). Thus it is not fully clear, whether the observed periods actually correspond to the rotation of the stellar surface; they might also be related to the rotation of the circumstellar matter in an accretion disk.

In contrast to this, the WTTS are surrounded by much less circumstellar material, many of them seem to be entirely "naked" (cf. Osterloh & Beckwith 1995, Wolk & Walter 1996). This means that we can expect to have neither accretion processes nor active disks. The photometric variations of the WTTS can be consistently explained by spots on the stellar surface that are 500 K to 1500 K cooler than the surrounding photosphere (Bouvier et al. 1995). These spots are probably the stellar analogons of sunspots and thus we can be rather confident that the photometric periods actually correspond to surface rotation.

2.1. Input data

The rotational data were taken from the compilation in Bouvier et al. (1995) and thus should represent a rather homogeneous data set. The stellar angular diameters have been calculated from the stellar luminosities and spectral types given by Strom et al. (1989), using the spectral type – effective temperature calibration from Cohen & Kuhi (1979) for the calculation of the stellar radii. Since we want to determine the distance, we need a quantity which is independent of the distance D assumed to calculate the luminosities (160 pc for the luminosities of Strom et al. 1989). So we will use the dimensionless and distance independent angular diameters $\phi := 2R_\star/D$.

It is important to note that the determination of stellar luminosities of T Tauri stars is not straightforward. Strom et al. (1989) have computed the luminosity of each star in two different ways. In the first method, the luminosity (denoted as $L_{\rm tot}$ in their paper) is determined by integrating over the spectral energy distribution. In the second method, they try to exclude all emission in excess of the spectral energy distribution expected for a main sequence star of the corresponding spectral type from the luminosity (denoted as $L_\star$ in their paper). Such a subtraction is certainly necessary and valid to estimate the actual stellar luminosities for the CTTS in their sample, which often show large excesses at infrared and UV wavelengths, most probably caused by accretion and massive active disks. However, the WTTS are neither accreting matter, nor do they possess active circumstellar disks. The small infrared excesses of the WTTS can be explained by other causes. For example, large cool spots on the stellar surface cause infrared excess emission. Strom et al. estimate that 20% – 50% spot coverage is needed to explain the observed excesses of their WTTS. They assume such a large spot coverage to be unrealistic, but we know that our WTTS actually have such large cool spots, because otherwise one would not find the strong modulations of the lightcurves which are the basis of the determination of the rotational periods. Bouvier et al. (1995) estimates a typical spot coverage of up to 30%, and this is just what is necessary to explain the observed infrared excesses. If this excess emission would be subtracted, the stellar luminosity would be clearly underestimated.

Since the K band excesses and the IRAS fluxes of our WTTS are rather small, these stars clearly do not possess large amounts of circumstellar matter. We therefore can be confident that the small infrared excesses are not caused by active disks or by accretion. A small amount of circumstellar matter around the WTTS might cause some infrared excess emission by absorbing stellar light and reemitting it at infrared wavelengths. Such an excess, however, should not be subtracted, since this is only reprocessed stellar radiation.

Another origin of an infrared excess could be binary companions. Of course it would be highly desirable to be able to subtract the luminosity of a possible companion, since the possible presence of unresolved binaries limits the accuracy of our distance estimate (see below). However, we have performed a detailed investigation of the excess-subtraction method used by Strom et al. and find that their method does not subtract the companion's luminosity. This is because Strom et al. adjust the model SED to the observed magnitude at R, and a stellar companion adds a significant contribution to the R magnitude of the system. The contribution of the companion would be very small only if the companion had a much lower surface temperature than the primary. The method of Strom et al. therefore will rather reliably subtract the luminosity of a brown dwarf companion with a surface temperature around 2000 K, but not for a

Table 1. Spectral types, rotation periods P, rotational velocities $v \sin i$, luminosities L (for an assumed distance of 160 pc), binarity information, and angular diameters ϕ for our sample of WTTS in the Taurus cloud. KFR is the K band flux ratio (defined as flux(companion)/flux(primary)) for known binaries, "ncd" means that no companion was detected in the Speckle survey of Leinert et al. (1993). Code for references: 1: Bouvier et al. (1995) and references therein, 2: Bouvier et al. (1993), 4: Johns-Krull (1996), 5: Prosser et al. (1995), 6: Hatzes (1995), 7: Leinert et al. (1993), 8: Ghez et al. (1993), 9: Strom et al. (1989)

Star	SpT	P [days]	$v \sin i$ [km/sec]	ref	L [$L_\odot$]	ref	companion?	KFR	ref	ϕ [10^{-10}]
HDE 283572	G5	1.55	95	1,4	9.88	9	ncd		7,8	9.1
HP Tau/G2	G0	1.20	79.5 ± 3	1,4	10.78	9	ncd		7,8	8.9
IW Tau	K7	5.60	6.9 ± 1.8	1	1.41	9	yes	0.91	7	5.0
LkCa 3	M1	7.20	21.8 ± 1.9	1	2.48	9	yes	0.68	7	8.5
LkCa 4	K7	3.37	26.1 ± 2.4	1	1.26	9	ncd		7	6.6
LkCa 7	K7	5.64	12.9 ± 2.9	1	1.15	9	yes	0.56	7	5.2
LkCa 14	M0	3.35	21.9 ± 1	1	0.93	1	ncd		7	5.9
LkCa 19	K0	2.24	18.6 ± 1.9	1	1.51	1	ncd		7	4.2
TAP 9	K5	1.60	20	1,2	0.59	9	yes	0.22	7	3.5
TAP 26	K7	0.55	68	1,5	0.56	9	ncd		7	4.4
TAP 35	K1	2.74	16	1	1.90	9	ncd		7,8	4.9
TAP 40	K5	3.38	17	1	0.44	9	ncd		7	3.2
TAP 41	K7	2.43	27	1	0.78	9	ncd		7	5.2
TAP 45	K7	6.20	11.5 ± 2.5	1	0.54	9	ncd		7	4.2
TAP 49	G8	3.32	12.2 ± 2.9	1	0.63	9	–			2.6
TAP 51S	F8	3.2	≤ 5	1	1.99	9	–			3.6
TAP 57NW	K7	9.3	10.4	1	1.26	9	ncd		7	6.6
UX Tau A	K2	2.7	25.4 ± 1.6	1	2.40	9	yes	0.07	7	6.1
V410 Tau	K3	1.87	71 ± 9.5	1,6	3.16	6	yes	0.16	8	9.5
V773 Tau	K2	3.42	55 ± 3.4	1	10.30	9	yes	0.13	7,8	11.9
V819 Tau	K7	5.6	≤ 15	1	1.03	9	yes	0.03	7	5.9
V826 Tau	K7	3.7	4.2 ± 0.7	1	2.20	9	ncd		7	8.9
V827 Tau	K7	3.75	18.5 ± 4.2	1	1.40	9	ncd		7	7.0
V830 Tau	K7	2.75	29.1 ± 2.4	1	1.05	9	ncd		7	6.1
V836 Tau	K7	7.0	≤ 15	1	0.85	9	ncd		7	5.4

stellar companion, which necessarily has a temperature above 3100 K.

For these reasons we use the "total" luminosity of Strom et al. This has the further advantage that this quantity is directly computed from the measured magnitudes and does not rely on any assumptions about the intrinsic colors of the WTTS, which are not well known. It might be interesting to note that for some stars Strom et al. find a "stellar luminosity" that is are even larger than the "total luminosity", demonstrating the problems of their excess-subtraction method.

2.2. The effect of binarity

It is well known that most stars are binaries, and this is also true for T Tauri stars (cf. Mathieu 1994). In an unresolved binary system we can be rather sure that the measured spectral type and rotational properties are those of the primary, since usually the primary dominates in the visible light. However, if we observe an unresolved binary system, the luminosity we find is the system luminosity and therefore we will systematically overestimate the stellar luminosity and hence the angular diameter, leading to an underestimate of the distance. It is therefore necessary to correct the luminosities and angular diameters for the effect of unresolved companions.

The multiplicity of our sample is very well studied since with only two exceptions all stars were included in the K band speckle imaging surveys of Leinert et al. (1993) and Ghez et al. (1993). These speckle observations could resolve companions down to separations of $0.13''$ ($\approx$ 20 AU at a distance of 160 pc) and 8 stars in our sample were detected to be binaries. Leinert et al. (1993) concluded that the binary frequency for the young stars in Taurus seems to be between 80% and 100%. So it is clear that most probably our sample of 25 stars contains a significant number of unresolved binaries.

For the 8 resolved binaries in our sample we have used the flux ratios found in the speckle observations to calculate a correction for the stellar angular diameters. The details of our correction procedure are given in the appendix. For the suspected unresolved binaries, however, we can only use a reasonable estimate of the binary frequency and perform simulations in order to estimate the possible systematic effect on our results. Before we do this, we will neglect the unresolved binaries for a moment and introduce our method in the next section. However, we note that the inferred distance will thus be a lower limit to

the true distance. In Sect. 5 we will investigate the effect of the suspected unresolved binaries on our results.

3. Method

If we assume that the photometric period is equal to the rotation period at the equator the quantities given in Table 1 are related by

$$\pi \, \phi \, D = P \, v \tag{1}$$

Since spectroscopic observations can only measure the projected velocity component $v \sin i$ and not the actual equatorial rotational velocity v, we have to use the relation

$$\pi \, \phi \, D \, \sin i = P \, [v \sin i] \tag{2}$$

where the parentheses around $[v \sin i]$ indicate that rotational velocity and inclination angle cannot be disentangled without further information.

Since we do not know the inclination angles for individual stars without knowing the distance, we obviously cannot derive any conclusions from this formula for individual stars. However, for a reasonably large sample of stars we can gain information from the distribution of inclination angles with the following strategy: We can calculate $\sin i$ values assuming some distance D and can compare the distribution of these $\sin i$ values with the expected distribution. Then we can vary the assumed distance until we find the best agreement between the expected and actual distribution.

To simplify the notation we define a new variable $S := \sin i$, which is given by

$$S(D) := \frac{P \, [v \sin i]}{\pi \, \phi \, D} \tag{3}$$

To calculate the expected distribution of this quantity, we assume the rotation-axes of the stars to be randomly orientated. In this case the theoretical distribution function $f(S)$ is given by

$$f(S) = S / \sqrt{(1 - S^2)} \qquad \text{for} \quad 0 \leq S \leq 1 \tag{4}$$

However, a comparison of the theoretical distribution with the distribution of the S values of our sample (calculated for the distance of 160 pc as assumed by Bouvier et al. 1995) shows that the two distributions disagree substantially (see Fig. 1): The shape of the distributions is significantly different; furthermore, some stars of our sample show $S > 1$, what should be impossible according to the theoretical distribution function.

The cause of this discrepancy can be easily uncovered: a distribution according to formula (4) can only be expected if all quantities involved were accurately known. In practice, however, all quantities are associated with measurement errors. These errors will cause systematic deviations of the observed distribution of S values from the theoretical distribution (4) and may also produce some S values exceeding unity.

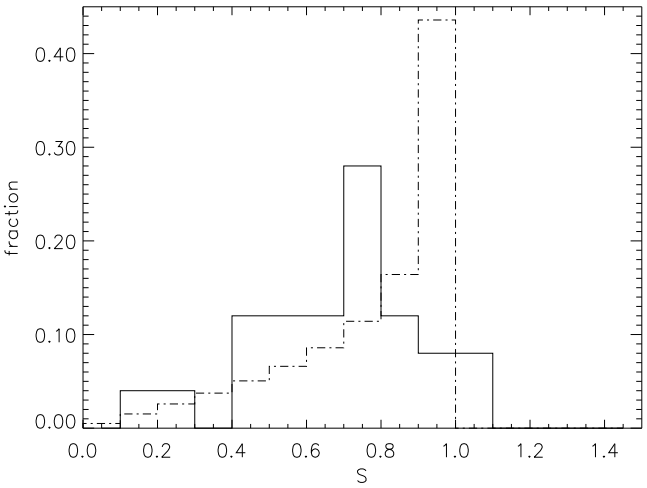

Fig. 1. Histogram comparison of the distribution of S values in our sample for an assumed distance of 160 pc (solid line) with the expected theoretical distribution according to formula (4) (dashed-dotted line).

A solution to this problem has been proposed by Hendry et al. (1993): The strategy is, to include the measurement errors into the theoretical model distribution. It is very difficult, if not impossible, to find an analytical formula for the model distribution $f(S)$ in the presence of measurement errors. However, we do not really need an analytical formula but can model this distribution by the use of Monte-Carlo simulations. To do this, we split the right side of Eq. (3) into two factors:

$$S(D) = \frac{P \, [v \sin i]}{\pi \, \phi \, D} = \frac{P_0 \, [v \sin i]_0}{\pi \, \phi_0 \, D} \times \frac{\frac{P}{P_0} \, \frac{[v \sin i]}{[v \sin i]_0}}{\frac{\phi}{\phi_0}} \tag{5}$$

Here P_0, $[v \sin i]_0$, and ϕ_0 are the (unknown) true values of these quantities, while P, $[v \sin i]$, and ϕ are the actually measured values, which are influenced by statistical measurement errors. Now, the first factor of (5) contains only the true values and thus obeys the theoretical distribution (4). The second factor contains the ratios of the true and the measured values and its distribution can be easily modeled in a Monte Carlo simulation.

3.1. Measurement errors

Before modeling the measurement errors we have to estimate their typical size. Our assumptions are based on the following facts:

The rotational periods can be determined rather accurately from the Fourier analysis of the light curves (see Bouvier et al. 1993, 1995). We assume the relative uncertainties to be about 5%. For the spectroscopic rotational velocities we assume relative uncertainties of 10%, as suggested by the errors given in Table 1.

For the angular diameters the estimation of the uncertainties is not so straightforward and we have to trace them back to the roots. The angular diameters are based on the stellar radii calculated from the luminosities and spectral types using the

Stefan-Boltzmann law $L_\star = 4\pi\,\sigma\,R^2\,T_{\rm eff}^4$. The luminosities, in turn, were determined from the magnitudes, the effective temperatures from the spectral types using the calibration from Cohen & Kuhi (1979). The typical uncertainties of the magnitudes given by Strom et al. (1989) are $\lesssim$ 0.1 mag. The uncertainties associated with the transformation from spectral type to effective temperature can be estimated by comparing the Cohen & Kuhi (1979) calibration with the more recent work of de Jager & Nieuwenhuijzen (1987). Such a comparison reveals differences of up to 150 K (see also the discussion in Martin et al. 1994), which might introduce uncertainties of $\approx 5\%$ for the radii. Taken together, we estimate the uncertainties for the radii and thus also for the angular diameters to be about 10%.

3.2. Selection effects

It is also important to be aware that our sample might be subject to selection effects. The main effect is that stars with inclination close to $i = 0^\circ$ will be effectively excluded due to two reasons: First, for small angles i the projected rotational velocity $v \sin i$ will be very small and thus hard to measure. Second, for such a nearly pole-on view of the stellar surface the rotational modulation due to dark spots will introduce only very small, hardly detectable changes in brightness. Thus as the inclination i approaches $i = 0^\circ$ it is increasingly difficult to measure both $v \sin i$ and P.

It is extremely difficult, if not impossible, to quantify this selection effect for our sample. However, it is possible to model this effect at least qualitatively by introducing a lower cutoff at $S_{\rm lim}$ to the S values in the model distributions.

3.3. Monte Carlo simulation of the model distribution

To simulate the model distribution we started with 10 000 S values obeying distribution (4). We assume the measurement errors to be independent and to obey a normal distribution. To simulate the second factor in (5) we computed the ratios as follows:

$$X/X_0 = 1 + \sigma_x\,\mathscr{R}$$

where X stands for any of the quantities P, $[v \sin i]$, or ϕ, and $\mathscr{R}$ is a random number drawn from a Gaussian distribution of zero mean and unit dispersion. The quantity σ is the factor that scales the random distribution to the typical uncertainties as given above.

Since the uncertainties in ϕ are partially caused by the uncertainties of the magnitudes, we note that the distribution of the errors might be a log-normal distribution rather than a normal distribution. However, if we take this into account, the effect on our results is absolutely negligible.

Finally, we model the selection effects by removing all objects with $S < S_{\rm lim}$ from the model distribution. We have tried various values for $S_{\rm lim}$ ranging from 0 to 0.5.

4. Results

4.1. Simple qualitative analysis

In order to illustrate the method we will now perform a qualitative comparison of the observed distributions of S values for various distances to the model distribution. The intention of this simple comparison is only to demonstrate the principle of our method. The model distribution used here assumes errors as given above and no selection effect ($S_{\rm lim} = 0$). In Fig. 2 we plot $S(D)$ distributions for several different assumed distances D and compare them to the model distribution. One can see that for assumed distances of 120 pc the observed S values are systematically to large, for 160 pc and 180 pc they are systematically to small and hence clearly inconsistent with the theoretical distribution. For an assumed distance of 140 pc, however, we find reasonable agreement without systematic differences between both distributions.

It is clear that such a visual comparison of the histograms can only provide a rough estimate on the "best fit" distance. Furthermore, while histograms are useful to visualize the distributions, the binning of data points into a histogram is alway associated with a loss of information and should be avoided. In order to perform a more thorough analysis, we will not use histograms but compare the cumulative distribution functions of the measured S values to the model distribution.

4.2. Quantitative statistical analysis

In order to have a quantitative measure of how well the model distribution reproduces the distribution of S values in our sample, we used a Kolmogorov-Smirnov (KS) test. A detailed description of this test can be found in Press et al. (1992), from where we also took the corresponding computer routines. The Kolmogorov-Smirnov test not only provides a quantitative measure of the agreement between both distributions, but also gives the probability of the null hypothesis, i.e. that the set of measured S values and the model sample of S values are drawn from the same distribution.

The distance for which the KS test null hypothesis probability ($P_{\rm KS}$) is maximal is denoted as "best fit distance" in the following. To find this best fit distance, we calculated the $S(D)$ values in our sample for a grid of assumed distances ranging from 100 pc to 200 pc in steps of 0.25 pc. Then, for each of these distances we performed the KS test.

In Sect. 3.1 we have tried to make a realistic estimate of the uncertainties of the individual quantities needed to compute the observed S values. However, we cannot exclude the possibility that we have over- or underestimated these uncertainties. In order to investigate the possible effect of this, we have performed tests by increasing or decreasing the modeled scatter by factors up to 2. Furthermore, we have also tested several different assumptions for a selection effect, varying $S_{\rm lim}$ between 0 and 0.5.

In all cases we could find a unique clear maximum of $P_{\rm KS}$ and for all models with $S_{\rm lim} \leq 0.3$ we could find a best fit $P_{\rm KS}$ above 99%. Increasing or decreasing the modeled scatter did

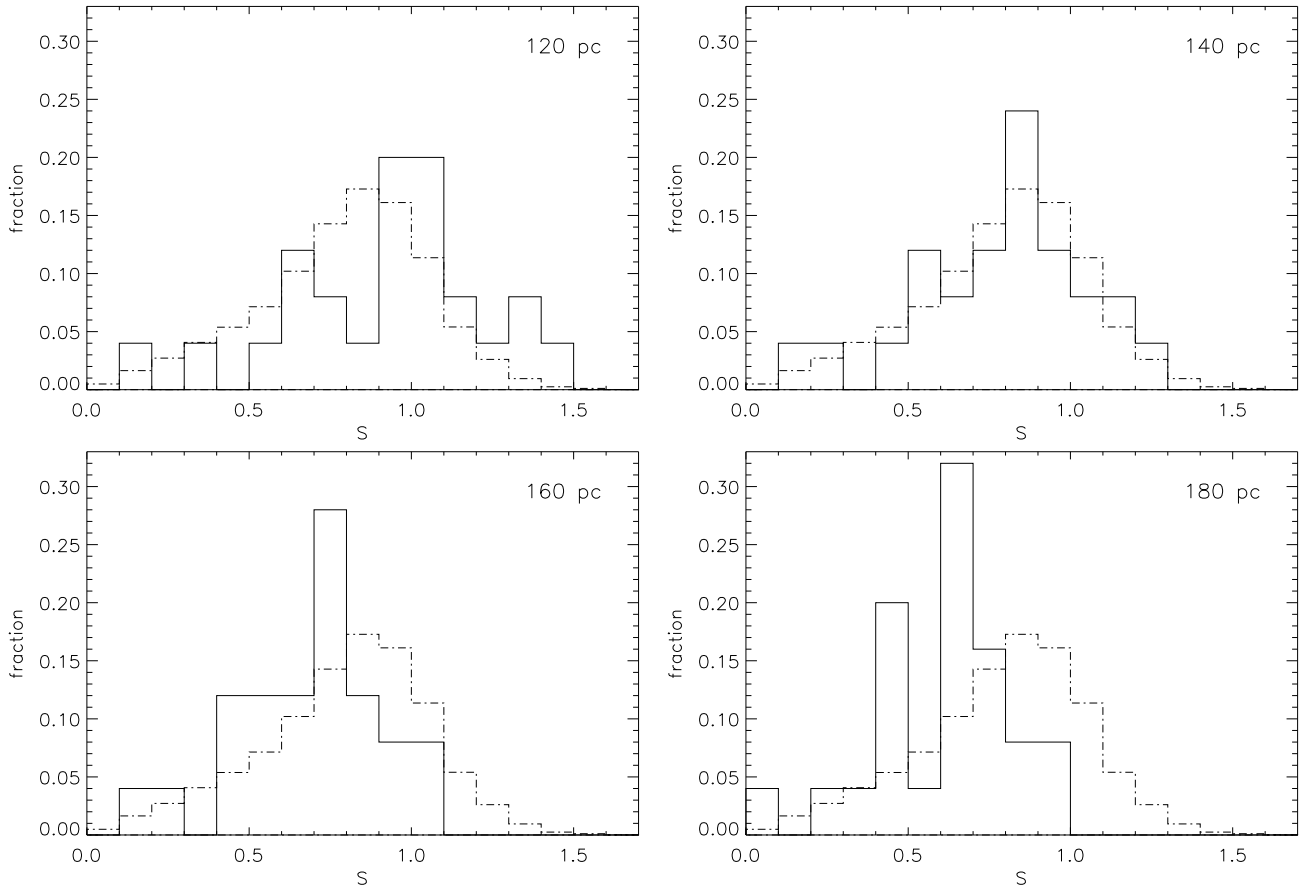

Fig. 2. Comparison of the distribution of the measured $S(D)$ values (solid line histogram) for different distances and the theoretical model distribution (dashed-dotted line histogram). For details see text.

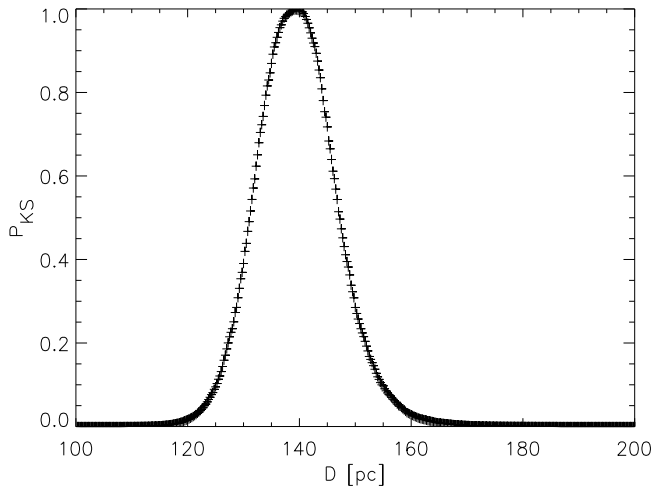

Fig. 3. Results of the Kolmogorov-Smirnov test on the observed versus model distribution for different distances (for details see text).

neither improve $P_{\rm KS}$ nor change the best fit distances significantly. This indicates that our estimation of the typical size of the uncertainties was good. All models with $S_{\rm lim} \leq 0.3$ gave very similar best fit $P_{\rm KS}$ values and also the best fit distances varied only slightly between 137 and 140 pc. These differences are not significant (see next paragraph). This shows that details of the assumed errors and selection effects have no significant influence on our results and proves the robustness of the method. We finally choose the model with $S_{\rm lim}$ = 0.15 that gives a best fit distance of 139.25 pc with $P_{\rm KS}$ = 99.7%. For this model we show $P_{\rm KS}$ as a function of the assumed distance in Fig. 3. In Fig. 4 we show the comparison of the cumulative distribution functions for the best fit distance.

4.3. Confidence limits from a Bootstrap analysis

Up to now we have only derived best fit distances. We still have to investigate the intrinsic uncertainties of this parameter estimation procedure. This can be done by simulating synthetic data sets and applying the same parameter estimation procedure to them as to the real data. The distribution of the parameter values resulting from the fits to the synthetic data sets can then be used as an approximation for the probability distribution of the actually found parameter values around the true value. This allows one to determine confidence limits on the estimated model parameter (cf. Babu & Feigelson 1996).

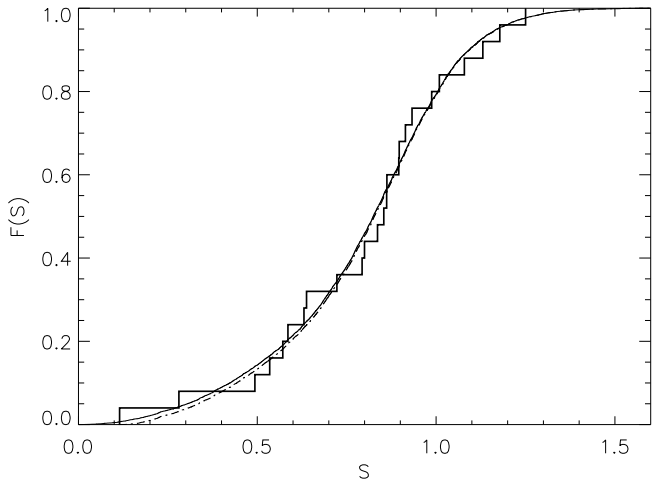

Fig. 4. Comparison of the cumulative distribution function $F(S)$ for the S values of our sample for a distance of 139 pc (thick solid line), for the model without selection effect (thin solid line) and for the model with a selection effect $S_{\rm lim} = 0.15$ (dashed dotted line).

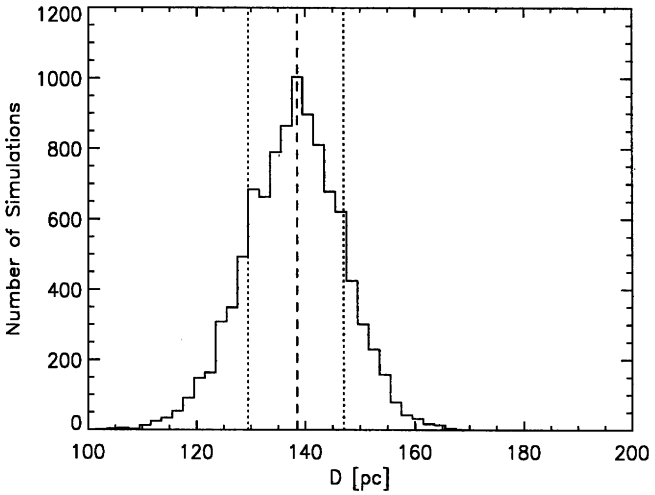

Fig. 5. Results of the bootstrap analysis: The histogram shows the distribution of the best fit distances found in 10 000 bootstrap simulations. The dashed line marks the median, the dotted lines are the boundaries of the 1σ confidence interval.

Since our sample is subject to selection effects and we do not precisely know the underlying errors, we will not try to model synthetic data sets. Instead, we will use the bootstrap method, in which synthetic data sets are obtained by drawing with replacement from the actual data set (cf. Press et al. 1992; Babu & Feigelson 1996). This assures that the synthetic data sets are subject to the same selection effects and errors as the actual data.

For our bootstrap simulations we generated 10 000 random samples, each containing 25 objects. For each of these synthetic samples we performed the same KS test analysis as for the actual data to derive the best fit distance. The results are shown in Fig. 5.

The median of the distribution of the distances found in the bootstrap procedure is 139 pc, in good agreement with the best fit distance from the actual data set. To determine the intrinsic uncertainties of the method we derive the 1σ confidence region as that interval centered on the median value that contains 68.3% of the resulting values. This interval extends from 130 pc to 147 pc and is bounded by the dotted lines in Fig. 5. We have performed the same bootstrap analysis for the other model distributions mentioned above and found very similar results in all cases.

Thus the intrinsic uncertainty of the parameter estimation procedure is about ± 8 pc. Since we have a small dependence of the best fit distance on the model assumptions of about ± 2 pc, the total error associated with our method is about ± 9 pc. It has to be emphasized that this is the intrinsic error of our statistical parameter estimation procedure. The actual uncertainty of the distance estimate is larger due to the uncertainties in the input data about the unresolved binaries as will be shown in the next section.

5. The effect of unresolved binaries

Only 8 stars in our sample are known to be binaries and have corrected angular diameters. However, it is rather obvious that our sample must contain some more unresolved binary systems, since 8 binaries out of 25 stars correspond to a binary frequency of only (32 ± 9)%. However, the multiplicity of nearby main sequence stars is between 40% and 60%, and the multiplicity of T Tauri stars in Taurus seems to be considerably higher and might be as large as 80 - 100% (cf. Leinert et al. 1993).

The probable presence of unresolved binaries can also be seen in the our data. If we determine the distance for the subsample of the 8 objects corrected for binarity, we find 146^{+14}_{-16} pc. If we use the subsample of the 17 unresolved stars we find a distance of 136^{+11}_{-12} pc. Although the difference is not statistically significant due to the large uncertainties caused by the small numbers in the subsamples, this is another indication that our result from the last section is only a lower limit to the true distance.

The only way to derive a more realistic distance estimate is to simulate the presence of additional binary systems among the unresolved stars in our sample. To do this, we have to specify the true binary frequency and the distribution function of the correction factors. The details of our simulation procedure are given in the appendix. We have generated 10 000 samples with simulated binary corrections, assuming a true binary frequency of 90%. The best fit distances found in this simulation show a rather narrow distribution with a median at 152 pc and a 1σ interval of ± 3.5 pc.

In order to check how strongly our assumptions about the unresolved binaries influence this distance, we varied the binary frequency and the distribution function of the corrections. For all reasonable assumptions, e.g. a binary frequency between 80% and 100%, the median of the best fit distances varied by not more than ± 2 pc. Thus we conclude that the total uncertainty

of our binary simulation procedure is ± 5 pc. Together with the intrinsic uncertainty of the parameter estimation (± 9 pc) we estimate a total uncertainty of ± 10 pc. So our best estimate for the distance of the T Tauri stars is 152 ± 10 pc.

6. Conclusions

Before drawing conclusions from our results, one has to be aware of the limitations of this method which mainly are caused by the underlying assumptions. Our method assumed a *common* distance for all stars in the sample. In reality, it is extremely improbable that all stars are actually exactly at the same distance. However, if there would be a significant scatter in the individual distances, our method should fail to find such a good agreement between the model and data. The high probabilities of more than 99% for the null hypothesis indicates that the scatter in distances is relatively small.

Our method is not well suited to derive good constraints on a possible scatter in distances, but we can at least try to find how sensitive the method is for a possible distance dispersion. In order to investigate this, we included an additional term in Eq. (5) that models a scatter in distances. As long as this scatter is smaller than about 10%, it affects the best fit probabilities and distances only very slightly[1]. However, if the distance scatter is increased above 10%, the best fit probabilities decreases noticeably. We therefore conclude that our method is sensitive to distance dispersion of about 10%. The actual scatter in distances is therefore probably less than 10%, since otherwise we would not expect to find such a good agreement with the assumption of a common distance.

We can use the projected spread on the sky to obtain at least a rough estimate on the possible scatter in distances. While the T Tauri stars in the Taurus region are now known to be widely distributed (Neuhäuser et al. 1995), the stars in our sample are tightly clustered around three clouds, L 1495, L 1536 and L 1551, separated by $\lesssim 10^\circ$. We thus find that at 150 pc, most of our stars are contained within a circle of radius ≈ 13 pc. This seems to be consistent with our upper limit to the distance dispersion of 10%.

Our result for the distance of 152 ± 10 pc is in good agreement with the range of distances between 140 pc and 160 pc used in recent work. However, it seems to be slightly larger than one of the most recent and reliable distance estimate for the molecular cloud material: In their spectrophotometric study Kenyon et al. (1994) find that most the molecular gas is at a common distance of 140 ± 10 pc. This suggests that the T Tauri stars lie within the cloud and not preferably at the near edge of the cloud.

There are two additional aspects we want to emphasize. The first aspect is that for a reasonably assumed distance our data are consistent with a distribution of randomly-orientated rotating stars. This means that there is no preferential orientation, which might be expected to occur e.g. due to the influence of large scale magnetic fields in the molecular cloud where the stars are forming. For several young stellar objects an apparent alignment of jets, outflows, or disk/envelope structures to the cloud magnetic field direction has been found (e.g. Tamura 1995). However, there is no evidence for a global alignment of outflows with the cloud magnetic field (for a discussion see Heiles et al. 1993). This is consistent with our result.

The second aspect is concerned with differential rotation. Isolated convective stars are expected to rotate differentially. If a star is differentially rotating and the spots producing the variations in the light curve are not on the equator, the photometric period would be different from the true rotational period and the method used here should fail (Smith 1994). However, since the method seems to work, this indicates that at least most stars in our sample are not strong differential rotators or the spots lie close to the equator. Confirmation of the spot locations may finally come through Doppler imaging techniques as well as modeling of the light curve variations (see Smith 1996).

Knowledge of the distance and inclination angles of these young stars is one step in testing our ideas on star formation. Firstly, the distance to very young CTTS and post T Tauri stars in the same region should soon be derivable. Secondly, spin axes can be compared with binary orbital rotation axes (e.g. Mathieu 1994) to constrain star formation theories.

Acknowledgements. MDS thanks the von Humboldt Foundation for financial support at the Max-Planck-Institut für Astronomie. It is a pleasure to thank Daniela Rohr, Melvin Hoare and J. Isserstedt for discussions and several helpful comments. This work was supported by the Deutsche Forschungsgemeinschaft through the Schwerpunkt Programm 'Physics of Star Formation' (grants Zi 242/10-1 and Yo 5/18-1).

Appendix A: determination of radius corrections from the speckle flux ratios

As explained in Sect. 2.1, the stellar luminosities given in Table 1 include the contributions of possible companions. Since the stellar radii are calculated from these luminosities, we have to correct for the contribution of the secondary in order to calculate radii for the primary stars correctly. The only information available for this correction is the K band flux ratio for the resolved binary systems from Leinert et al. (1993) or Ghez et al. (1993), defined as KFR = flux(companion)/flux(primary). We assume that the stars in a binary system are coeval, i.e. they lie on an isochrone. We use the isochrone data from the model calculations of D'Antona & Mazzitelli (1994) with CM convection and Alexander opacities to simulate binaries. Each data point on an isochrone corresponds to a star for which we know the luminosity L and the effective temperature T. We assume that the stellar radius is related to these quantities by the Stefan-Boltzmann law, thus we have

$$R = R_\odot \times \sqrt{\frac{L}{L_\odot}} \left(\frac{T^2}{T_\odot^2} \right)^{-1}$$

The problem with this method is that the photometry of an unresolved binary system gives the system luminosity, which is the

[1] It might be worth mentioning that the best fit probabilities always decrease when adding a scatter in distances.

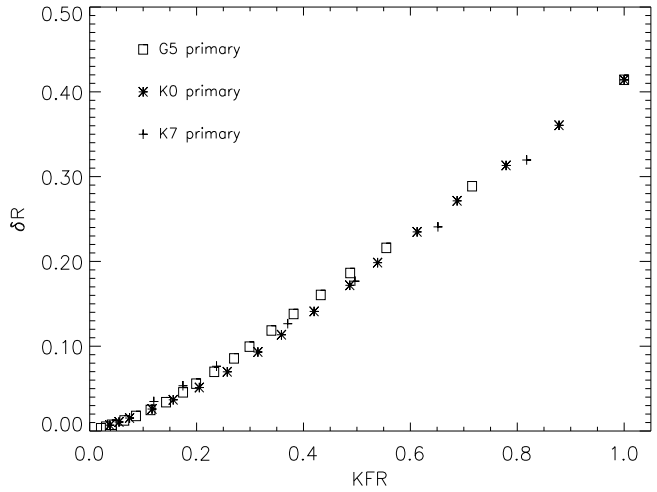

Fig. 6. The relation between the observed flux ratio KFR in the K band and the radius correction for different binary systems (for details see text).

sum of the primary and secondary luminosity, $L_p + L_s$. In most binary systems the primary dominates the optical spectrum. So the measured spectral type is that of the primary. In systems in which both components have (nearly) equal luminosities, the companion necessarily has (nearly) the same spectral type as the primary, so this should not introduce any significant errors. So we can be rather sure that the measured spectral type and thus the effective temperature is that of the primary. Thus, the "radius" we find from the observational data for an unresolved binary system is

$$R_t = R_\odot \times \sqrt{\frac{L_p + L_s}{L_\odot}} \left(\frac{T_p^2}{T_\odot^2}\right)^{-1}$$

obviously an overestimation of the actual stellar radius of the primary. The relative overestimation of the primary radius R_p is

$$\delta R := \frac{R_t - R_p}{R_p}$$

From the isochronal data we can easily compute this quantity. If we assume some data point of the isochrone to be the primary star, all other data points for lower mass stars at the same isochrone are the possible companions of this primary. For each possible binary system we calculated δR. It is also straightforward to calculate the K band flux ratio for each of these systems by assuming the stars radiate like black bodies.

In Fig. 6 we show the results of our calculations for binary systems with three different primaries. These data are based on the 3 Myr isochrone, which should be rather representative for the young stars in Taurus. The 1 Myr isochrone gives nearly identical results. This relation between KFR and δR can be used to correct the radii of the primary stars in the known binary systems of our sample.

Appendix B: simulated corrections for unresolved binaries

Most probably, a large fraction of the stars in our sample which were unresolved in the speckle observations nevertheless are binaries. We can take this into account by simulating radius corrections for some of the unresolved stars. This requires two assumptions. The first is the probability with which we apply such a correction to an unresolved star. This probability can be easily calculated from the assumed true binary frequency for the total sample. For example, if we assume the true binary frequency to be 90% and take into account that 8 of the 25 stars are already known binaries, this probability for each of the 17 unresolved stars to be a binary is P_b = 85.3%.

The other assumption is how to calculate simulated radius corrections. Leinert et al. (1993) show that the distribution of flux ratios found in their sample is consistent with the assumption that both components of each binary system have been drawn independently from a Miller-Scalo initial mass function. The distribution of flux ratios shown in Fig. 6b of Leinert et al. (1993) can be approximately modeled by a simple Gaussian distribution of unit standard deviation in the interval $0.05 \leq KFR \leq 1$.

Our simulation procedure works as follows. From our original sample we construct 10 000 simulated samples by randomly applying binarity corrections to the radii of the unresolved stars. This is done by first drawing a number from a uniform distribution between 0 and 1. If this number is less then P_b, we simulate a correction factor by drawing a number from a Gaussian distribution. If this number is outside the interval between 0.05 and 1, another number is drawn. It is then used as the flux ratio, and the radius correction factor is calculated from the $KFR - \delta R$ relation shown in Fig. 6.

In order to check how sensitive the results of this procedure depend on our assumptions, we varied the width of the Gaussian distribution by factors between $1/2$ and 2 (this results in distributions which are either more strongly peaked towards low flux ratios, or are flatter) and we also varied the lower limit of the distribution of flux ratios between 0.02 and 0.1.

References

Babu, G.J. & Feigelson, E.D., 1996, *Astrostatistics*, Chapman & Hall, London
Bouvier, J. & Bertout, C., 1992, A&A 263, 113
Bouvier, J., Cabrit, S., Fernandez, M., Martin, E.L., Matthews, J.M., 1993, A&A 272, 176
Bouvier, J., Covino, E., Kovo, O., Matthews, J.M., Terranegra, L., Beck, S.C., 1995, A&A 299, 89
Camenzind, M., 1990, in: *Reviews in Modern Astrononmy 3*, ed. G. Klare, p. 234
Cernicharo, J., Bachiller, R., Duvert, G., 1985, A&A 149, 273
Cohen, M. & Kuhi, L.V., 1979, ApJS 41, 743
D'Antona, F. & Mazzitelli, I., 1994, ApJS 90, 467
de Jager, C. & Nieuwenhuijzen, H., 1987, A&A 177, 217
Eislöffel, J., 1992, J.H., Ph. D. thesis, Heidelberg
Elias, J.H., 1978, ApJ 224, 857
Ghez, A.M., Neugebauer, G., & Matthews, K., 1993, AJ 106, 2005
Gomez, M., Jones, B.F., Hartmann, L., et al., 1992. AJ, 104, 762

Hatzes, A.P., 1995, ApJ 451, 784
Heiles, C., Goodman, A.A., McKee, C., & Zweibel, E.G., 1993, in: *Protostars and Planets III*, eds. E.H. Levy & J.I. Lumine, University of Arizona Press, p. 279
Hendry, M.A., O'Dell, M.A., Collier Cameron, A., 1993, MNRAS 265, 983
Johns-Krull, C.M., 1996, A&A, 306, 803
Kenyon, S.J., Dobrzycka, D., Hartmann, L., 1994, AJ 108, 1872
Kenyon, S.J. & Hartmann, L., 1995, ApJS 101, 117
Leinert, Ch., Zinnecker, H., Weitzel, N., et al., 1993, A&A, 278, 129
Martin, E.L., Rebolo, R., Magazzu, A., & Pavlenko, Y.V., 1994, A&A 282, 503
Mathieu, R.D., 1994, ARA&A 32, 465
Montmerle, T., 1990, in: *Reviews in Modern Astrononmy 3*, ed. G. Klare, p. 209
Neuhäuser, R., Sterzik, M.F., Schmitt, J.H.M.M., Wichmann, R. & Krautter, J., 1995, A&A 297, 391
O'Dell, M.A., Hendry, M.A., Collier Cameron, A., 1994, MNRAS 268, 181
Osterloh, M. & Beckwith, S.V.W., 1995, ApJ 439, 288
Press, W.H., Flannery, B.P., Teukolsky, S.A. & Vetterling, W.T., 1992, *Numerical Recipes*, Cambridge University Press
Prosser, C.F., Shetrone, M.D., Dasgupta, A., et al., 1995, PASP 107, 211
Racine, R., 1968, AJ 73, 233
Smith, M.D., 1994, A&A, 287, 523
Smith, M.D., 1996, In proc. Disks & Outflows Around Young Stars, ed. S. Beckwith & J. Staude, p. 323
Strom, K.M., Strom, S.E., Edwards, S., Cabrit, S., Skrutskie, M.F., 1989, AJ 97, 1451
Tamura, M., Hough, J.H., & Hayashi, S.S., 1995, ApJ 448, 346
Valenti, J.A., Basri, G., Johns, C.M.,, 1993, AJ 106, 2024
Walter, F.M., Brown, A., Linsky, J.L., et al., 1987, ApJ 314, 297
Walter, F.M., Brown, A., Mathieu, R.D., Myers, P.C., Vrba, F.J., 1988, AJ 96, 297
Wolk, S.J. & Walter, F.M., 1996, AJ 111, 2066

This article was processed by the author using Springer-Verlag LaTeX A&A style file *L-AA* version 3.